Direct Observation of a Self-Affine Crack Propagation

Jean Schmittbuhl
Laboratoire de Géologie, URA 1316, École Normale Supérieure, 24 Rue Lhomond, 75231 Paris Cedex 05, France

Knut Jørgen Måløy
Fysisk Institutt, Universitetet i Oslo, P.O. Boks 1048 Blindern, N-0316 Oslo 3, Norway
(Received 28 October 1996)

We study experimentally the propagation of an in-plane crack through a transparent Plexiglas block. The toughness is controlled artificially and fluctuates spatially like uncorrelated random noise. The system is loaded by an imposed displacement and cracks in mode I at low speed (10^{-7}–5×10^{-5} m/s). The crack front is observed optically with a microscope and a high resolution digital camera. During the propagation, the front is pinned and becomes rough. Roughness of the crack front is analyzed in terms of self-affinity. The roughness exponent is shown to be 0.55 ± 0.05 in a static regime. No evolution of the roughness exponent is observed during the propagation even if the crack speed changes. [S0031-9007(97)03193-1]

PACS numbers: 62.20.Mk, 46.30.Nz, 61.43.–j, 81.40.Np

As first mentioned by Mandelbrot *et al.* [1], the geometry of fractured surfaces exhibits scaling invariance. Numerous works have shown the self-affine properties of crack surfaces [2–6]. The roughness exponent is found to be very robust over different materials, different fracture modes [3], and a broad range of length scales. This range can be extended if earthquake faults are considered as fractured surfaces [2,7]. The estimate of the roughness exponent is close to 0.80. A possible "universal" self-affine crack geometry of heterogeneous material has been proposed by Bouchaud *et al.* [3]. In other words, the crack surface presents a geometrical property which is independent of the actual quenched disorder of the toughness in the material. However, the physical origin of the very long range spatial correlations leading to *self-affinity* along fractured surfaces is not fully understood.

Most theoretical studies of this problem are based on a simple argument: The geometry of the crack surface is the inheritance of the crack front geometry during the fracture propagation. The front line has a three-dimensional structure. The component along the mean plane of the fracture is labeled as the in-plane roughness. Perpendicular to this plane, the front has an out-plane roughness. Only the latter constructs the roughness of the crack surface. However, in-plane and out-plane roughnesses are not independent [8]. Long range correlations along the front may explain long range correlations within the surface. Two directions are being explored. A Langevin equation has been proposed by Bouchaud *et al.* [8] keeping only terms allowed by the symmetry of the system. With this approach only local terms and an annealed noise are considered for the evolution of the system. The second approach has been initiated from the work of Rice [9,10]. It includes a nonlocal kernel resulting from the elasticity in the bulk. Noise in this case is a spatial fluctuation of the toughness. It is quenched. Because of the complexity of the elastic Green function, mainly in-plane cracks have been studied for a propagation in a heterogeneous medium. In the quasistatic regime [11], the front is shown to be self-affine with a roughness exponent of 0.35. A study of the dynamic propagation is proposed by Perrin and Rice [12,13]. The quasistatic limit of a similar model is obtained by Ramanathan *et al.* [14]. In the case of a mode I crack, they predict a transition from logarithmic correlations at large scales to a self-affine scaling at small scales. The crossover scale is a function of the crack speed. At low speed, the self-affine regime is expected to be dominant.

The relevance of a specific crack model is difficult to estimate owing to the lack of experimental observations. Direct observation of the crack front is usually impossible and an inverse description of the crack front obtained for instance from acoustic emissions is generally observed with a low spatial resolution. Daguier *et al.* [15] proposed a first experimental roughness characterization of a crack front propagation in a randomly heterogeneous medium. Using ink, they casted the crack tip at a given stage of the propagation. It is a three-dimensional casting from which they extracted the self-affine exponent describing the in-plane roughness of the crack: $\zeta = 0.60$. Mower and Argon [16] were able to capture directly the propagation of a crack in a transparent epoxy containing defaults as nylon rods. However, in this case, defaults are not randomly distributed.

We report in this Letter on the experimental observation of in-plane crack fronts which propagate in a block of polymethylmethacrylate. Fronts are directly observable because of the transparency of the material. The Plexiglas block is made with two plates of Plexiglas-GS: $L = 32$ cm $\times$ $l = 14$ cm $\times$ $h = 1$ cm that are annealed together at 200 °C under several bars of normal pressure. The annealing surface corresponds to a weak toughness plane. Before the merging process, random flaws are

 0031-9007/97/78(20)/3888(4)$10.00

introduced artificially by sandblasting the surfaces with 50 μm steel particles. With this surface treatment, the Plexiglas becomes unpolished and looses its transparency. The magnitude of the roughness along the Plexiglas surface is lower than a few micrometers. Using a microscope, we checked the random position of the maximum defaults. The structures observed have a cutoff around 50 μm. As seen below this is much smaller than long range correlations observed in the power spectrum of the fronts (see Fig. 3) which extend up to the size of the image (5 mm). Sandblasting creates height fluctuations which influence locally the toughness and makes it fluctuate from place to place. The Plexiglas has viscoelastic properties. Mechanical tests were performed to characterize the rheology of the material. The elastic modulus is estimated as $E = 3.3$ GPa. The viscous behavior is obtained by a relaxation test. The relaxation modulus decreases logarithmically with time (between one sec and one hour) which suggests that numerous time scales are involved in the viscous response.

A fracture propagates within the weak plane of the Plexiglas block along the direction L when plates are separated with a mechanical press by imposing a displacement δ (along the h direction). The contact between the press and the Plexiglas plate is nonrigid. A rod pulls the plate and friction is reduced by adding oil. The crack propagation is in mode I and stable. No mode II or III is introduced. During the propagation, the front is pinned by local regions of high toughness and becomes rough. The geometry of the crack front is observed with a microscope. A digital camera set on the top of the microscope provides high resolution images: 1536 $\times$ 1024 pixels (4.8 μm per pixel). Using a specifically developed software, we extract the front path as a $z(x)$ function (see Fig. 1). The front is defined as a contrast boundary between the cracked area which appears as nontransparent (i.e., unpolished) and the cracked area which is transparent (i.e., annealed). The annealing procedure suppresses the light scattering due to the roughness. A perfect contact exists everywhere between the Plexiglas plates. Areas with no contact will be easily seen as nontransparent islands within transparent regions. Moreover these islands are expected to increase with applied stresses. No such effects are observed. The Plexiglas block is lying on a balance with a high dynamic resolution (1 mg–1 kg). It provides a force measurement during the crack propagation. The mechanical press is moved with a stepping motor (10^{-4} mm/step). A computer controls the experiment by monitoring the mechanical press, the trigger of the digital camera, and the record of the force measurement with the balance.

Figure 2 shows the load-displacement history during an experiment as the measurement of the force F acting on the plate (linearly dependent on the mass m provided by the balance) with respect of the imposed displacement δ. Assuming an elastic rheology of the Plexiglas plate, a straightforward expansion leads to

$$F(\delta, \bar{z}) \propto E \frac{\delta}{\bar{z}^3}, \tag{1}$$

where E is the Young modulus and $\bar{z}$ the average position of the front. The linear evolution on the graph probes the elastic rheology of the system since the force is proportional to the displacement δ for a constant position of the crack. After some threshold in the force acting on the system, the front moves forward and crack surface is produced. Dissipation resulting from surface creation relaxes the mechanical energy stored in the system. This process is visible in Fig. 2 as the departure from the linear evolution. Crack dissipation becomes very efficient and spends the mechanical energy faster than provided by the load. It corresponds to the maximum and the decrease of the loading force on the curve.

Two classes of experiments are distinguished. The first class corresponds to static situations. A crack is propagated as described above. After several millimeters of propagation, the system is maintained at a constant imposed displacement δ. The crack stops and is observed

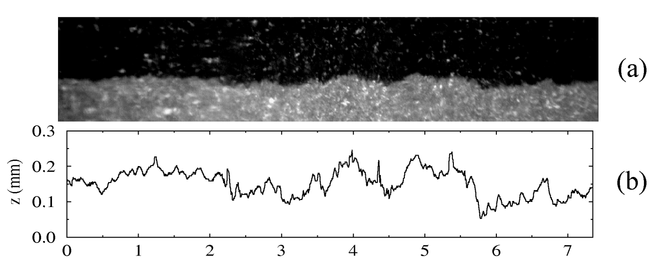

FIG. 1. Sample of a crack front. (a) is the raw image where the intact material appears as black. In contrast, the cracked zone is white. Crack propagates in this case from bottom to top because of a tensile load. (b) is the front path extracted from (a) after image treatment. It is defined as a $z(x)$ function.

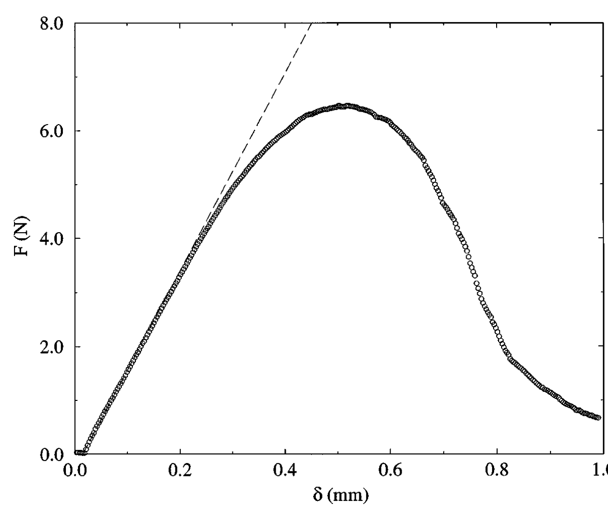

FIG. 2. A high dynamic balance is set under the crack propagation setup and measures the force F acting on the plate. Shown is the evolution of the force when a displacement δ is imposed. The crack is initiated when the curve leaves the linear elastic behavior.

at that stage. The second class of experiments concerns dynamic evolution of cracks for a nonconstant load.

We first study the crack front roughness for static experiments. We analyze 89 pictures. Some of the pictures are not independent. They show the same front in the same position. Differences in this case provide a quantification of the error bars due to the experimental setup for visualization (camera, microscope, lighting, etc.).

The self-affine geometry of the front is estimated by three independent techniques described in Ref. [17]. The variable bandwidth method is the computation of the root mean square σ and the maximum-minimum differences d of the z component of the front over windows of size Δ. Both quantities are expected to scale as $\sigma(\Delta) \propto \Delta^{\zeta}$ and $d(\Delta) \propto \Delta^{\zeta}$, where ζ is the roughness exponent. We measure $\zeta = 0.50$ for the root mean square technique and $\zeta = 0.62$ for the maximum-minimum difference. The second method is the computation of the return probability $P(d_0)$. It is the histogram of the distances d_0 needed to find back the same height as the starting one. Actually, we use a logarithmic binning to improve the readability of the method. The probability behaves as $P(d_0) \propto d_0^{\zeta-1}$. We obtain in this case $\zeta = 0.52$. The last method is the estimate of the Fourier spectrum which scales as $P(f) \propto f^{-1-2\zeta}$. The latter provides an estimate of $\zeta = 0.54$. According to Ref. [17], Fourier analysis should provide the most accurate absolute value of the self-affine exponent. Results for this method are presented in Fig. 3. The synthesis of the different estimates, taking into account systematic biases, leads to

$$\zeta = 0.55 \pm 0.05 . \tag{2}$$

Eventual local ill descriptions of the front path may appear owing to a local poor contrast in the raw image of the front. The use of different analysis techniques that converge to the same result probes the weak influence of such experimental artifacts.

During dynamic experiments, digital pictures are taken regularly (every 10 s). Figure 4 presents 27 steps of the front evolution. The front is initiated from a main default and accelerates with time. The average speed of the front is estimated from the computation of the mean position of the front and from the trigger time of the pictures. It is confirmed by the force measurement during time. Using Eq. (1), the instantaneous position of the front $\overline{z}(t)$ is determined and the speed v deduced. The magnitude of crack speed varies from 10^{-7} to 5×10^{-5} m/s. Roughness of the front is analyzed with the same techniques as mentioned above. For each recorded step of the propagation (i.e., each profile), the roughness exponent is measured and the instantaneous speed evaluated. Figure 5 presents estimates of the roughness exponent averaged over the different self-affine analysis techniques as a function of the speed of the crack. No evolution of the roughness exponent ζ is observed taking into account error bars of the measurements. The error bars are larger than for static experiments since self-affine analyses in the case of dynamic experiments are done on a single profile and not on a set of profiles. From Fig. 5, we conclude that the roughness exponent estimated from static experiments is conserved during the propagation of the crack. The evolution of the roughness magnitude has also been studied during the propagation. No major trend has been observed.

In the system described above, crack propagation takes place within a plane and no roughness is left in the cracked

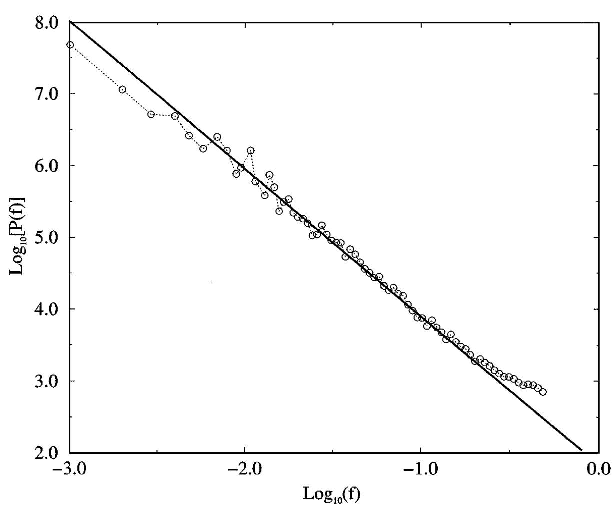

FIG. 3. Power spectrum of the crack front for static experiments. The average over 89 profiles is shown. Slope of the spectrum provides an estimate of the roughness exponent: $\zeta = 0.54$.

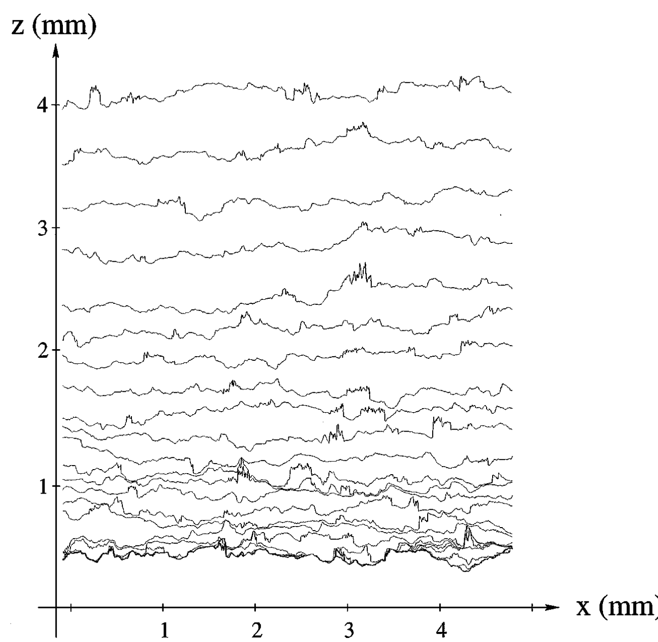

FIG. 4. 27 steps of the crack front evolution during a dynamic experiment. Steps are separated by 10 s. The front is initiated from a main default (on the right bottom of the picture) and propagates from bottom to top. The complete horizontal field of the picture corresponds to a distance of 5 mm. The vertical axis has been stretched by a factor of 1.5 to increase the readability.

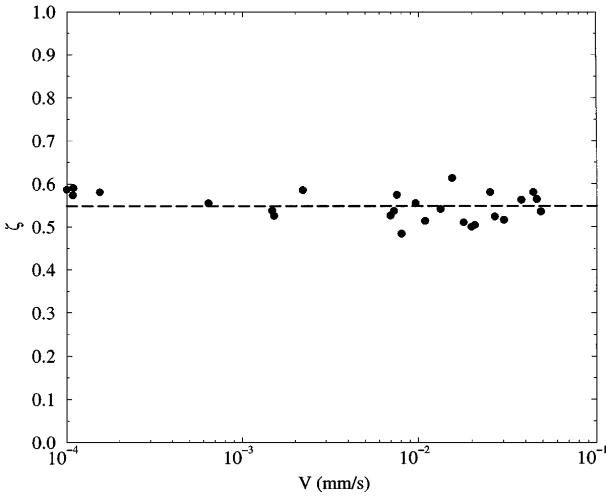

FIG. 5. Roughness evolution during propagation for a single dynamic experiment. The roughness exponent ζ is plotted with respect to the average speed of the crack v. Different techniques of roughness analysis are used: Fourier spectrum, return probability, maximum-minimum difference, and root mean square. Estimates of the roughness exponent are averages over the different techniques. Fluctuations exist around the static value of the roughness exponent 0.55 but no clear evidence of velocity dependence is shown over almost 3 orders of magnitude.

surface. We focus on the roughness of the crack front and obtain a value of the self-affine exponent consistent with the results of Daguier *et al.* [15] where the propagation is really three dimensional and the range of speeds is comparable (around 10^{-10} times the sound speed). Independence of the roughness exponent with the crack speed is of special interest for the study of crack speed influence. Crack speed is responsible for the onset of instabilities which initiates roughness. Experimental results concern mainly the case of homogeneous materials and two-dimensional systems [18,19]. For heterogeneous material, only slow (i.e., far from the speed of sound) experiments have been done. Bouchaud and Navéos [20] show that roughness scaling of the crack surface is a function of the crack speed. The crack speed controls a crossover length scale between two different scalings of the roughness. On a very different material (sandstone), Plouraboué *et al.* [21] obtained a completely independent scaling with crack velocity in the range 5×10^{-4} to 2×10^{-1} m/s.

The roughness of crack surfaces may have two origins: the heterogeneity of the medium and the speed of the crack. This study confirms experimentally that heterogeneities are important if combined with bulk properties of the medium. Surrounding volume of the crack front introduces long range correlations. A crack front which propagates in a uncorrelated random medium is self-affine as shown either from models containing only nonlocal elastic terms [11,14] or purely local terms [8,22]. The measured roughness exponent is 0.55 for a slow crack propagation in mode I which is not fully consistent with any models. Otherwise, we show that the roughness exponent is independent of the crack speed even if time scales resulting from the viscous rheology or the dynamics of local openings are involved.

A better collapse of experimental and theoretical results is expected if several aspects are considered in models of slow propagation (i.e., far from Rayleigh speed). Ramanathan *et al.* [14] suggested that the load mode influences drastically the spatial correlations along the crack front. Moreover, the viscous behavior of the material may involve a large range of time scales and modified effective spatial correlation lengths. The influence of the chemical composition of the atmosphere around the crack tip should be studied in order to check the potential influence of chemical reactions on the crack process.

We thank S. Roux, J. P. Vilotte, and E. G. Flekkøy for very useful discussions. This work has been supported by the Groupement de Recherche "Géoméchaniques des Roches Profondes."

[1] B. B. Mandelbrot, D. E. Passoja, and A. J. Paullay, Nature (London) **308**, 721 (1984).
[2] S. R. Brown and C. H. Scholz, J. Geophys. Res. **90**, 12 575 (1985).
[3] E. Bouchaud, G. Lapasset, and J. Planès, Europhys. Lett. **13**, 73 (1990).
[4] B. L. Cox and J. S. Y. Wang, Fractals **1**, 87 (1993).
[5] K. J. Måløy, A. Hansen, E. L. Hinrichsen, and S. Roux, Phys. Rev. Lett. **68**, 213 (1992).
[6] J. Schmittbuhl, F. Schmitt, and C. H. Scholz, J. Geophys. Res. **100**, 5953 (1995).
[7] J. Schmittbuhl, S. Gentier, and S. Roux, Geophys. Res. Lett. **20**, 639 (1993).
[8] J. P. Bouchaud, E. Bouchaud, G. Lapasset, and J. Planès, Phys. Rev. Lett. **71**, 2240 (1993).
[9] J. R. Rice, J. Appl. Mech. **52**, 571 (1985).
[10] H. Gao and J. R. Rice, ASME J. Appl. Mech. **56**, 828 (1989).
[11] J. Schmittbuhl, S. Roux, J. P. Vilotte, and K. J. Måløy, Phys. Rev. Lett. **74**, 1787 (1995).
[12] G. Perrin and J. Rice, J. Mech. Phys. Solids **42**, 1047 (1994).
[13] J. R. Rice, Y. Ben-Zion, and K. Kim, J. Mech. Phys. Solids **42**, 813 (1994).
[14] S. Ramanathan, D. Ertas, and D. S. Fisher (unpublished).
[15] P. Daguier, E. Bouchaud, and G. Lapasser, Europhys. Lett. **30**, 367 (1995).
[16] T. Mower and A. Argon, Mech. Mater. **19**, 343 (1995).
[17] J. Schmittbuhl, J. P. Vilotte, and S. Roux, Phys. Rev. E **51**, 131 (1995).
[18] J. Boudet, S. Ciliberto, and V. Steinberg, Europhys. Lett. **30**, 337 (1995).
[19] J. Fineberg, S. Gross, M. Marder, and H. Swinney, Phys. Rev. B **45**, 5146 (1992).
[20] E. Bouchaud and S. Navéos, J. Phys. I (France) **5**, 547 (1995).
[21] F. Plouraboué *et al.*, Phys. Rev. E **53**, 277 (1996).
[22] S. Roux and A. Hansen, J. Phys. I (France) **4**, 515 (1994).